

GEOMETRIC ACCURACY ASSESSMENT OF MSG-SEVIRI LEVEL 1.5 IMAGERY

Sultan Kocaman Aksakal, Emmanuel Baltsavias, Konrad Schindler

ETH Zurich, Institute of Geodesy and Photogrammetry
CH-8093 Zurich, Switzerland
sultan.aksakal@geod.baug.ethz.ch, emmanuel.baltsavias@geod.baug.ethz.ch,
konrad.schindler@geod.baug.ethz.ch

Abstract

The geometric accuracy of the images acquired by the SEVIRI (Spinning Enhanced Visible and Infra-Red Imager) instrument aboard the European geostationary satellites Meteosat-8 (formerly MSG-1) and Meteosat-9 (formerly MSG-2) has been investigated in this study. Level 1.5 image data of the High-Resolution Visible (HRV) band with 1-km Ground Sample Distance (GSD) and several multispectral (MS) bands with 3-km GSD at sub-satellite point have been provided by the Swiss GCOS Office at MeteoSwiss. A set of fully automated processing methods has been adopted, developed and implemented for the evaluation of relative and absolute accuracy of the HRV images and band-to-band registration (BBR) accuracy between the HRV and 6 MS channels. Details of the relative and absolute accuracy evaluation methods and the results have been published in Aksakal (2013) and Aksakal et al. (2013) and briefly given in this paper. The methodology for the assessment of BBR accuracy and the results are provided first time here. SEVIRI images acquired in 2008 have been analyzed and relative and absolute shifts of up to 10 pixels have been observed in the images which were acquired from Meteosat-8. The BBR errors are found within the specifications given by EUMETSAT.

INTRODUCTION

GCOS (Global Climate Observing System) is a long-term program undertaken by several international organizations for monitoring the climate, detect changes, and assess their impacts (GCOS, 2013). The Swiss GCOS Office at the Federal Office of Meteorology and Climatology (MeteoSwiss) is responsible for coordinating GCOS activities in Switzerland (Seiz et al., 2011). Satellite images are being increasingly used for climate-related measurements and derivation of Essential Climate Variables (ECVs). Satellites are particularly suited for wide-area, repetitive observations of the Earth, even over areas that are difficult to access (Swiss GCOS Office, 2013; WMO, 2011). Under a research agreement between the Swiss GCOS Office and ETH Zurich, the geometric accuracy of image products acquired from three different satellite sensors (SEVIRI aboard the European meteorological satellites of the Meteosat Second Generation Series, MODIS aboard the NASA satellites Terra and Aqua, AVHRR aboard the NOAA and Metop satellite series), which are often used to estimate ECVs, are being investigated. Such investigations are essential, since geometric errors modify the location and possibly extent of derived climate variables and conclusions about their change. An example on the impact of band-to-band misregistration errors for MODIS Aqua can be found in Arnold et al. (2010). GCOS has also defined target requirements for geometric accuracy (WMO, 2011).

The project aims at investigating: a) the relative geometric accuracy within one image, between different channels, and for multi-temporal imagery; b) the absolute geometric accuracy using reference data; c) the temporal stability of the absolute as well as the relative geometric accuracy; d) the impact of geometric errors on the derivation of climate variables. In particular, we investigate whether the geometric accuracy specifications of the related sensor products are really fulfilled over Switzerland. In the first stage of the project, the geometric accuracy of the SEVIRI has been investigated. The SEVIRI instrument is designed to support nowcasting, numerical weather forecasting, and climate applications

over Europe and Africa (Aminou et al., 2003). The instrument generates images of the Earth in 12 different spectral channels aboard Meteosat-8 and Meteosat-9. During the period selected for investigations, SEVIRI aboard Meteosat-9 was in operation as the main instrument and Meteosat-8 was used as stand-by. The Level 1.5 data of SEVIRI consist of georeferenced, calibrated and radiance-linearized information for the derivation of meteorological products and other meteorological processing (Eumetsat, 2010; Just, 2000). The geometric accuracy specifications for SEVIRI Level 1.5 data from Meteosat-8 and Meteosat-9 are: < 3.0 km for absolute, < 1.2 km for relative between two consecutive images, and 0.6 km (within the VNIR and HRV channels) and 1.5 km (for all channels) for BBR (EUMETSAT, 2007).

There have been a few studies in the literature reporting the geometric accuracy of the SEVIRI imagery (Hanson et al., 2003; Hanson and Müller, 2004; Gieske et al., 2005; Dürr and Zelenka, 2009). The methods used for the relative and absolute geometric accuracy investigations in this study and the test results are provided in detail in Aksakal (2013) and Aksakal et al. (2013). The BBR accuracy assessment methods and results are provided here together with a summary and comparison of the relative and absolute accuracy.

METHODOLOGY

In order to achieve the project goals, a set of fully automated processing methods has been adopted, developed and implemented (Aksakal, 2013; Aksakal et al. 2013). For relative accuracy assessment, a large number of features are extracted and tracked through the images of the same day, using the KLT (Kanade-Lucas-Tomasi) tracker (Lucas and Kanade, 1981) extended with statistical analysis and blunder detection procedures to ensure a robust evaluation without matching errors. To assess absolute accuracy, lakes in the area are used as reference and the lake boundaries are matched in the images via 2D sub-pixel translations. For the BBR assessment, two different methods are used for the evaluation of HRV and MS channels and the details are provided below.

Relative Accuracy Evaluation

The relative accuracy is evaluated in terms of 2D translation errors for sequences of consecutive HRV images acquired on the same day. For each day selected for processing, 17 images acquired between 9:00-13:00 UTC are used. The processing steps for the relative accuracy investigations with the HRV channel data are given in detail in Aksakal (2013) and Aksakal et al. (2013). A large number of ($\approx 300-1000$) feature points are extracted from the first image of the day (9 o'clock) and matched in the consecutive image (i.e. taken at 9:15) using the KLT tracker. The given HRV cloud masks are integrated in the point selection process in order to exclude cloud regions. After matching, statistical values are calculated from all points based on the image coordinate differences with signs ($\Delta x, \Delta y$): *Mean*, *standard deviation* (σ), *median* (*MED*), *median absolute deviation from the median* (*MAD*), *min*, and *max* values. Every ($\Delta x, \Delta y$) is compared against the *mean-x* and *mean-y*, respectively; and the ones having an absolute difference larger than 3σ are considered as outliers. The *MED* and *MAD* values are used for a final comparison with the *mean* and σ values, in order to analyze existence of any remaining outliers in the dataset ($\sigma \approx 1.48 * MAD$). The blunders usually occur in low contrast and low texture areas and are caused by matching errors. The outlier check is repeated iteratively until a blunder-free set is obtained. The matching process continues until the last image of the day, which is selected as 13:00 image for this evaluation. Successfully matched points are used as candidate points for the next pair of images (e.g. 9:15 and 9:30). If the total number of points after the blunder detection falls below a given threshold, new points are added to the candidate list based on the earlier image of the new pair and the cloud mask. In practice, the total number of points is usually above 500 and the percentages of matching outliers are in the range of 3%-20%, with an average of 10%.

Absolute Accuracy Evaluation

Absolute accuracy evaluation of the SEVIRI imagery is done based on lakes in HRV images, since the detection of shorelines is relatively easy and reliable and lakes are the only detectable objects with a good contrast to the land. The approach is based on the observation that the pixel grey values of the lakes in the images are low (typically less than 30), and the water pixels are always darker than the

surrounding lake-shores. Larger lakes in the area are manually digitized into vector polygons from two different Landsat orthophotos and used as reference and transformed into the HRV image space (Aksakal, 2013). For the matching, each lake polygon is moved inside a 20x20 pixels search window (i.e. ± 10 pixels) starting from its initial position. A coarse-to-fine matching is performed in two steps: first, 1 pixel step size is applied to have an approximate matching; and second, the results obtained from the first matching are refined within a range of 1.2x1.2 pixels (i.e. ± 0.6 pixels). For the fine matching, a step size of 0.1 pixel is selected in order to achieve sub-pixel accuracy. At each step, the normalized sum of pixel intensities inside the lake polygons is computed. The partial pixels at the polygon edges are also added to the sum with respect to the pixel area that falls inside the polygon. The minimum of the normalized sums is selected for each lake within a given image. The step parameters, which provide the minimum sum, are considered the shift of the lake. The statistical values (*mean*, σ , *MED*, *MAD*, *min*, *max*) are derived from the shifts of all lakes in an image. After initial experiments, lakes having a cloud cover >40% are excluded from the process, since the matching is usually not successful (Aksakal et al. 2013).

Band-to-Band Registration Accuracy Evaluation

The HRV and 6 MS channels of SEVIRI are analyzed in terms of BBR accuracy. The MS channels are: VIS 0.6 (reflectance of 0.6 μm visible channel), VIS 0.8 (reflectance of 0.8 μm visible channel), IR 1.6 (reflectance of 1.6 μm near-infrared channel), IR 3.9 (brightness temperature of 3.9 μm infrared channel), IR 10.8 (brightness temperature of 10.8 μm infrared channel), and IR 12.0 (brightness temperature of 12.0 μm infrared channel). The BBR accuracy is evaluated using two different approaches. First, the BBR accuracy between the HRV and the VIS 0.8 channel images is evaluated based on the lake matching method, which is used for the absolute accuracy evaluation of HRV images. This method is selected due to the resolution difference between the HRV and VIS 0.8 channels. The lake matching is applied to the VIS 0.8 channel and the results are compared against the shifts of the HRV channel images of the same day and time. The lake matching process for the VIS 0.8 images has been slightly altered via: a) reducing the number of lakes to 10 due to smaller GSD (3 km); b) transforming the lake polygons into the image space of VIS 0.8; c) reducing the window size (6x6) for coarse matching; and d) integrating the cloud mask provided for the MS images.

Second, the KLT tracker method, which is used also for relative accuracy investigation of the HRV images, is employed for the matching of 6 MS images. VIS 0.8 channel is used as reference and the other 5 channels from the same acquisition are compared against it. Although the lakes are better visible in the IR 1.6 channel, its matching with the other MS channels is more difficult due to radiometric differences especially in the Alpine region. Due to significant local and global radiometric differences between the images, a number of image pre-processing methods have been applied. The processing steps for the BBR assessment of MS images are:

1. Wallis filter is applied to all 6 images in order to increase the contrast and similarity of the images, by forcing the mean and contrast of an image to fit to some given target values (Wallis, 1976).
2. Sobel edge filter is applied to Wallis-filtered images to enhance the edges. Even though the radiometric differences between the images are high, the edges usually remain the same. In addition, a histogram threshold (50%) is applied in order to remove weak edges (possibly due to noise).
3. The feature points are selected in the VIS 0.8 channel and matched in the other 5 channels using the KLT tracker. The cloud masks of MS channels are integrated in the process to ensure that no feature points are generated in the cloud regions. The cloud regions in the masks are extended by 2 pixels, in order to prevent generation of feature points at the cloud boundaries. The window size used in the tracker is selected as 70 x 70 pixels since the matching is more successful and robust with a larger window.
4. The results are inspected using the following criteria and the feature points are removed from the set if their matching is unsuccessful:
 - a. Matching status indication of KLT tracker in Python (1 or 0) is used to remove failed points.
 - b. Regional elimination via cross correlation (CC) criterion: Each image is divided into 6 regions (2x3 grid), and the best 65%-75% of the points in each region are used in the process depending on the total number of the points in the region. The CC value is used for each point as quality criterion. The patch size used to compute the CC value is 70 x 70.
 - c. Points having a CC value <0.6 are eliminated.

d. The statistical values are calculated for the remaining point set based on the image coordinate differences with signs ($\Delta x, \Delta y$): *Mean*, σ , *MED*, *MAD*, *min*, and *max* values. Similar to the relative accuracy evaluation process of HRV images, outliers are detected and removed from the point set based on a comparison between the image coordinate differences and the standard deviations. The statistical parameters are recalculated after outlier removal.

RESULTS AND DISCUSSION

Since the main aim is to analyze geometric accuracy over Switzerland, image parts covering a rectangular area over Switzerland and surrounding countries with a size of 652 x 393 pixels for HRV and 221 x 134 pixels for MS channels have been used. The HRV and VIS 0.8 image parts acquired on 30.08.2008 at 12:00 UTC and lakes used for absolute accuracy evaluation can be seen in Figure 1. Although the images have been acquired mainly from Meteosat-9 in 2008, there is a substantial amount of imagery from Meteosat-8 throughout the year. In addition, gaps have occurred in the image sequences on several days. Initial relative and absolute accuracy investigations have been performed using the HRV images from 24 different days (two days from each month with minimum cloud coverage) in 2008 (Aksakal, 2013). Due to large relative shifts (up to 8 pixels) between consecutive images on several days, further relative accuracy investigations have been performed using the images of additional 103 days. The BBR accuracy is investigated for the same acquisitions (24 days at 12:00) as for absolute accuracy evaluation.

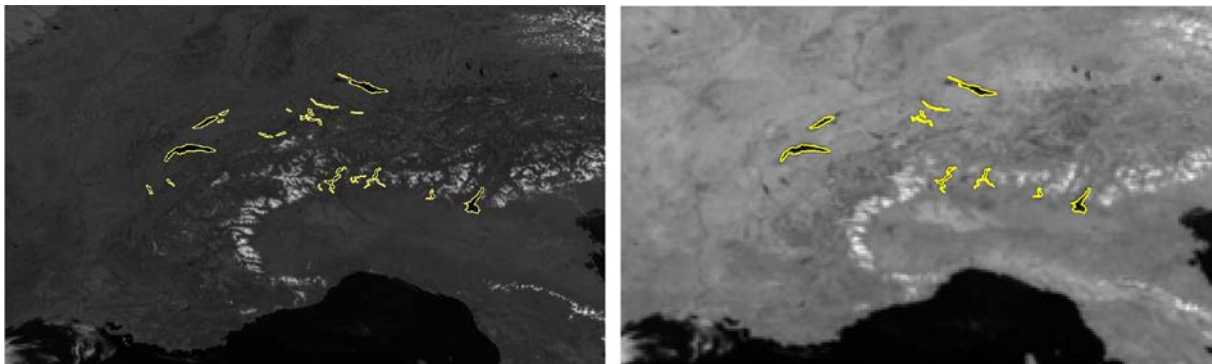


Figure 1. HRV (left) and VIS 0.8 (right) image parts (at different zoom levels) from 30.08.2008 and the lakes used for absolute accuracy investigations.

Relative Accuracy Investigations

The relative accuracy of HRV images are investigated using a total of 2111 HRV images acquired on 127 days, between 9:00-13:00 UTC. There have been gaps on some days due to high cloud cover or data unavailability. The results are provided for Meteosat-8 and Meteosat-9 in Table 1. In addition, the HRV data of 4 days, where the image sequences contain data from both satellites, have been analyzed separately and the results are provided in the lower part of the Table. The number of points matched in image pairs for all days is in the range of 211-1037, with an average of 570.

The results of Meteosat-8 are obtained from the images of 24 days. The *Min* and *Max* values for the $Mean_x$ and $Mean_y$ of Meteosat-8 data show that the relative shifts occur in all directions. However, the variations are larger along the y axis (up to 9.6 pixels). The minus sign shows shifts to West and South for x and y, respectively. The *Mean* and *MED* values of the shifts are quite similar, showing that no big blunders exist in the results. The mean σ_x and σ_y are slightly less than 0.1 pixels, which can be considered as matching accuracy. The higher σ (up to 0.30 pixels) occurred on cloudy days, which causes more matching errors. In the results of Meteosat-9 in Table 1, shifts up to 0.31 and -1.39 pixels for x and y are observed. The *mean* σ values obtained from all pairs are around 0.1 pixels as in the Meteosat-8 results. In comparison to Meteosat-8, the relative accuracy of Meteosat-9 is better, i.e. the geolocalization is more stable. The parameters computed from the images of 4 days, on which multiple satellite swaps have occurred, show shifts up to -0.99 (x) and 1.42 (y) pixels. The larger shifts have occurred during the swaps, where a pair is composed of one Meteosat-8 and one Meteosat-9 image. Figure 2 shows the relative shifts obtained over 127 days. The main observation is that large

shifts are present between 01.02.2008-19.02.2008, and only when Meteosat-8 was in operation as primary mission. On later days, also Meteosat-8 delivers stable images.

| Satellite | Value | Mean (x) | Mean (y) | MED (x) | MED (y) | σ (x) | σ (y) | MAD (x) | MAD (y) |
|------------------------|-------|--------------|--------------|---------|---------|--------------|--------------|---------|---------|
| Meteosat-8 | Min | -1.20 | -9.59 | -1.20 | -9.59 | 0.03 | 0.02 | 0.02 | 0.01 |
| | Max | 1.13 | 9.42 | 1.14 | 9.44 | 0.28 | 0.30 | 0.17 | 0.16 |
| | Mean | -0.04 | 0.06 | -0.04 | 0.06 | 0.07 | 0.08 | 0.04 | 0.05 |
| Meteosat-9 | Min | -0.30 | -1.39 | -0.30 | -1.39 | 0.03 | 0.02 | 0.02 | 0.02 |
| | Max | 0.31 | 0.77 | 0.33 | 0.77 | 0.30 | 0.30 | 0.17 | 0.18 |
| | Mean | -0.02 | -0.01 | -0.02 | -0.01 | 0.11 | 0.12 | 0.06 | 0.08 |
| Meteosat-8& Meteosat-9 | Min | -0.99 | -0.39 | -1.00 | -0.42 | 0.03 | 0.04 | 0.02 | 0.03 |
| | Max | 0.86 | 1.42 | 0.87 | 1.39 | 0.21 | 0.23 | 0.14 | 0.16 |
| | Mean | -0.06 | 0.01 | -0.07 | 0.01 | 0.06 | 0.09 | 0.04 | 0.06 |

Table 1. Statistical summary of the relative shifts from all image pairs for all 127 days (in HRV pixels).

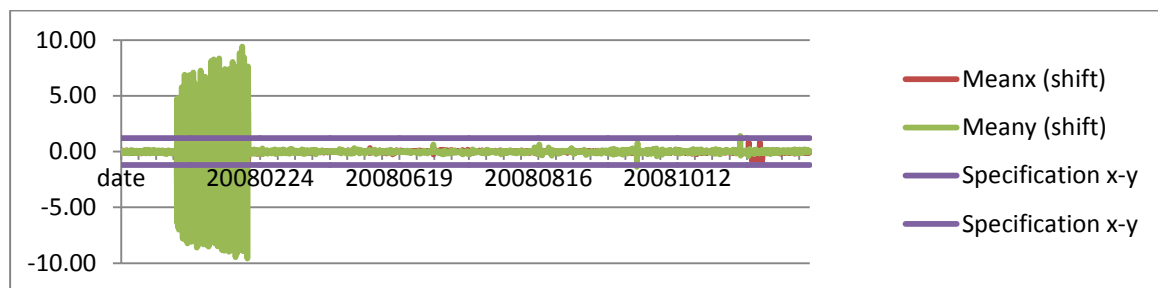


Figure 2. Relative shifts (in pixels) obtained from the images acquired on 127 days between 9:00-13:00 in 2008 and the accuracy specification of EUMETSAT. The horizontal axis denotes the date.

Absolute Accuracy Investigations

The lake matching is applied to the HRV images acquired on 24 different days (two days from each month) at 12:00 and the results are summarized in Table 2. Positive values indicate shifts to the North and East, respectively. The range for the number of lakes used for the Meteosat-9 evaluations is 6-20, with a mean of 16, the variations being caused by clouds. For Meteosat-8, the number of lakes ranges from 12-19, with a mean value of 17. Figure 3 shows zoomed images with different lakes. It can be seen in Figures 3b and 3c that lakes partially covered by clouds can also be used for the evaluations. The statistical values given in Table 2 for Meteosat-8 are derived from the estimated shift values of individual lakes for 5 days. All images are shifted to North and East. The variation in y is larger, between 0.3 and 3.3 pixels, showing poorer stability of the sensor in this direction. The σ values calculated from the individual lake offsets are in the range of 0.1-0.3 pixels, with a mean σ of 0.2 pixels, which shows the mean accuracy of the matching. This value can also be interpreted as the variability of absolute accuracy among the lakes of one image. The *Min*, *Max*, *Mean* and *MED* values in Table 2 for Meteosat-9 are derived from the lake matching results of 19 days. Again, all images are shifted to North and East, with a max shift of 1.4 pixels for x and 3.0 pixels for y. Similar to the Meteosat-8 results, the mean σ values are in the range of 0.1-0.3 pixels, with a mean of 0.2 pixels. When the results of both satellite datasets are compared, no significant accuracy differences have been observed between the two satellites. However, it should be noted that the results given in Table 2 have been obtained from the 12:00 images only. The large relative shifts (up to 10 pixels, see previous section) imply also large absolute accuracy errors (Aksakal et al., 2013).

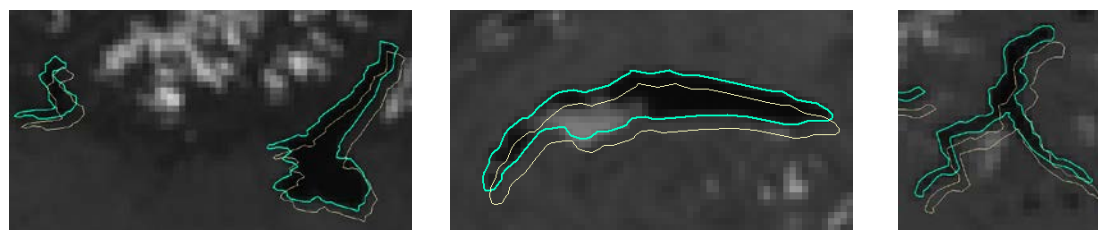


Figure 3. a) Iseo and Garda Lakes (left); b) Lemano Lake (middle); and c) Como Lake (right). The yellow and green polygons denote the initial positions and the matched positions.

| Satellite | | Mean (x) | Mean (y) | Mean (xy) | σ (x) | σ (y) | MED (x) | MED (y) | MAD (x) | MAD (y) |
|------------|------|------------|------------|-----------|--------------|--------------|---------|---------|---------|---------|
| Meteosat-8 | Min | 0.5 | 0.3 | 0.9 | 0.1 | 0.2 | 0.5 | 0.3 | 0.1 | 0.1 |
| | Max | 1.5 | 3.3 | 3.3 | 0.2 | 0.3 | 1.4 | 3.3 | 0.2 | 0.2 |
| | Mean | 1.0 | 1.9 | 2.3 | 0.2 | 0.2 | 1.0 | 1.9 | 0.1 | 0.2 |
| | MED | 0.9 | 2.0 | 2.4 | 0.2 | 0.2 | 0.9 | 2.0 | 0.1 | 0.2 |
| Meteosat-9 | Min | 0.3 | 1.8 | 2.1 | 0.1 | 0.1 | 0.4 | 1.7 | 0.0 | 0.1 |
| | Max | 1.4 | 3.0 | 3.1 | 0.3 | 0.3 | 1.3 | 3.0 | 0.1 | 0.2 |
| | Mean | 0.9 | 2.3 | 2.5 | 0.2 | 0.2 | 0.9 | 2.3 | 0.1 | 0.1 |
| | MED | 1.0 | 2.2 | 2.4 | 0.2 | 0.2 | 1.0 | 2.2 | 0.1 | 0.1 |

Table 2. Absolute accuracy evaluation; statistical summary from the shifts of 12:00 images.

Band-to-Band Registration Accuracy Evaluation Results

The lake matching is applied to the 12 o'clock images of the VIS0.8 channel on 24 days in order to calculate the absolute geolocation errors and to provide a comparison with the HRV images taken at the same day and time, providing indirectly BBR accuracy between HRV and MS images. Since lake matching was obstructed on one day due to cloud cover on large lakes, the comparison is based on the absolute shifts of VIS 0.8 and HRV images of 23 days (Table 3). The mean shifts of HRV images are reduced by the a factor of 3, which is the ratio of the GSDs of both channels, before the comparison and the BBR error of an image is calculated via:

$$\Delta x = \text{Mean}_{\text{vis0.8}} - \text{Mean}_{\text{hrv}}/3$$

$$\Delta y = \text{Mean}_{\text{vis0.8}} - \text{Mean}_{\text{hrv}}/3$$

| | Meteosat-9 | | Meteosat-8 | |
|----------------------------|-------------|-------------|-------------|-------------|
| | Δx | Δy | Δx | Δy |
| Min | -0.03 | -0.17 | -0.10 | 0.00 |
| Max | 0.20 | 0.07 | 0.13 | 0.07 |
| Mean | 0.11 | 0.02 | 0.03 | 0.02 |
| σ | 0.07 | 0.06 | 0.11 | 0.03 |

Table 3. BBR accuracy results (in MS pixels) between the VIS 0.8 and HRV channels of SEVIRI aboard Meteosat-8 and Meteosat-9. The comparison is based on the lake matching results.

The lake matching accuracy for the VIS 0.8 channel images is between 0.1-0.2 (min-max) pixels, with a mean of 0.1 pixels. The numbers of lakes used for the evaluations are in the range of 3-10, and the variations are caused by the clouds. The requirement of EUMETSAT for the BBR accuracy between the VNIR and the HRV channels is 0.6 km (0.2 MS pixels). The *min* and *max* values provided in Table 3 confirm that the BBR accuracy obtained from the investigations is within the specifications for the HRV and VIS 0.8 channels.

The BBR accuracies of SEVIRI's 6 MS bands (VIS 0.6, VIS 0.8, IR 1.6, IR 3.9, IR 10.8, IR 12.0) are evaluated using the 12:00 images of the 24 days (Table 4). The VIS 0.8 channel is used as reference for the other 5 channels for matching. The PN0 and PN1 in Table 4 show the numbers of the initial and successfully matched points, respectively. The spatial distributions of the points are mainly affected by the cloud cover. The *Mean*, σ , *MED*, and *MAD* values are obtained from the coordinate differences of the matched points. The *min*, *max*, and the *mean* values given in Stats (3rd col.) are derived from all image pairs for the corresponding band and satellite. 4 image pairs out of all 120 are removed from the process due to low number of successfully matched points (i.e. <5). All results in Table 4 are within the specifications for both satellites. The largest deviation for Meteosat-8 occurred between VIS 0.8-IR 3.9 (0.49 pixels to the North). In the analysis of the matching results, it has been observed that the larger shifts in y direction occurred on two days and only with IR 3.9, IR 10.8, and IR 12.0 channels. The shifts of the VIS 0.6 and IR 1.6 channel images are below 0.2 pixels in both directions. Regarding Meteosat-9, the shifts are up to 0.2 pixels for all bands and acquisitions, except for one day. On this day, the shift between VIS 0.8 and IR 10.8 is -0.35 pixels, and the shift between VIS 0.8 and IR 12.0 is -0.38 pixels both in y direction. The pair VIS 0.8-IR 3.9 could not be evaluated for this date as the matching was not successful. It should be noted that the cloud cover of this image is relatively high (~60%) and the spatial distribution of the points is poor.

| Band | Satellite | Stats | PN ₀ | PN ₁ | Mean _x | Mean _y | σ_x | σ_y | MED _x | MED _y | MAD _x | MAD _y |
|---------|-----------|-------|-----------------|-----------------|-------------------|-------------------|-------------|-------------|------------------|------------------|------------------|------------------|
| VIS 0.6 | Met-9 | min | 19 | 8 | -0.11 | -0.03 | 0.02 | 0.03 | -0.12 | -0.03 | 0.02 | 0.02 |
| | | max | 106 | 72 | 0.07 | 0.11 | 0.12 | 0.13 | 0.07 | 0.11 | 0.08 | 0.08 |
| | | mean | 55.3 | 30.2 | -0.04 | 0.04 | 0.06 | 0.07 | -0.03 | 0.04 | 0.04 | 0.04 |
| | Met-8 | min | 40 | 28 | -0.11 | -0.02 | 0.02 | 0.01 | -0.10 | -0.02 | 0.01 | 0.01 |
| | | max | 63 | 42 | 0.02 | 0.06 | 0.06 | 0.05 | 0.02 | 0.07 | 0.04 | 0.03 |
| | | mean | 52.4 | 36.6 | -0.04 | 0.03 | 0.04 | 0.03 | -0.04 | 0.04 | 0.02 | 0.02 |
| IR 1.6 | Met-9 | min | 19 | 15 | -0.15 | -0.08 | 0.03 | 0.03 | -0.15 | -0.09 | 0.02 | 0.02 |
| | | max | 106 | 72 | -0.04 | 0.06 | 0.10 | 0.09 | -0.05 | 0.06 | 0.07 | 0.06 |
| | | mean | 55.3 | 36.7 | -0.11 | -0.02 | 0.06 | 0.06 | -0.11 | -0.02 | 0.04 | 0.04 |
| | Met-8 | min | 40 | 13 | -0.17 | -0.16 | 0.05 | 0.07 | -0.17 | -0.16 | 0.03 | 0.05 |
| | | max | 63 | 41 | -0.05 | 0.03 | 0.13 | 0.12 | -0.05 | 0.06 | 0.06 | 0.09 |
| | | mean | 52.4 | 26.6 | -0.10 | -0.02 | 0.08 | 0.09 | -0.09 | -0.02 | 0.04 | 0.07 |
| IR 3.9 | Met-9 | min | 23 | 11 | -0.23 | -0.19 | 0.03 | 0.05 | -0.23 | -0.19 | 0.01 | 0.02 |
| | | max | 106 | 54 | 0.07 | 0.03 | 0.18 | 0.14 | 0.04 | 0.04 | 0.17 | 0.13 |
| | | mean | 57.4 | 22.6 | -0.10 | -0.08 | 0.09 | 0.08 | -0.10 | -0.08 | 0.06 | 0.05 |
| | Met-8 | min | 40 | 15 | -0.25 | -0.49 | 0.05 | 0.06 | -0.25 | -0.57 | 0.04 | 0.04 |
| | | max | 63 | 27 | 0.00 | -0.09 | 0.10 | 0.20 | -0.01 | -0.09 | 0.08 | 0.12 |
| | | mean | 52.4 | 21.8 | -0.13 | -0.22 | 0.08 | 0.12 | -0.13 | -0.25 | 0.06 | 0.07 |
| IR 10.8 | Met-9 | min | 19 | 8 | -0.17 | -0.35 | 0.04 | 0.03 | -0.17 | -0.34 | 0.02 | 0.03 |
| | | max | 106 | 57 | -0.03 | 0.02 | 0.13 | 0.14 | -0.05 | 0.01 | 0.11 | 0.13 |
| | | mean | 55.2 | 26.6 | -0.11 | -0.09 | 0.08 | 0.09 | -0.11 | -0.10 | 0.05 | 0.06 |
| | Met-8 | min | 40 | 19 | -0.24 | -0.44 | 0.04 | 0.07 | -0.23 | -0.45 | 0.02 | 0.07 |
| | | max | 63 | 41 | 0.00 | -0.12 | 0.13 | 0.14 | 0.00 | -0.10 | 0.08 | 0.12 |
| | | mean | 52.4 | 26.0 | -0.13 | -0.25 | 0.07 | 0.11 | -0.13 | -0.24 | 0.05 | 0.08 |
| IR 12.0 | Met-9 | min | 19 | 8 | -0.12 | -0.38 | 0.04 | 0.04 | -0.12 | -0.37 | 0.02 | 0.02 |
| | | max | 106 | 57 | 0.03 | 0.04 | 0.12 | 0.13 | 0.01 | 0.02 | 0.10 | 0.13 |
| | | mean | 55.2 | 26.1 | -0.05 | -0.08 | 0.08 | 0.09 | -0.05 | -0.09 | 0.05 | 0.06 |
| | Met-8 | min | 40 | 19 | -0.16 | -0.43 | 0.04 | 0.06 | -0.15 | -0.46 | 0.03 | 0.04 |
| | | max | 63 | 41 | 0.09 | -0.12 | 0.10 | 0.16 | 0.09 | -0.07 | 0.06 | 0.11 |
| | | mean | 52.4 | 26.0 | -0.06 | -0.24 | 0.07 | 0.11 | -0.04 | -0.24 | 0.04 | 0.07 |

Table 4. BBR accuracy results (in MS pixels) between the VIS 0.8 channel and 5 other MS channels of SEVIRI. The images are acquired on 24 different days at 12:00 UTC.

CONCLUSIONS AND FUTURE WORK

Under a research agreement with the Swiss GCOS Office, a set of algorithms for the geometric accuracy evaluation of SEVIRI Level 1.5 channel imagery is developed and tested. Images of HRV and 6 MS channels acquired from the SEVIRI instruments aboard Meteosat-8 (MSG-1) and Meteosat-9 (MSG-2) have been used for the investigations. Only the images acquired over Switzerland and surroundings in 2008 are evaluated. The proposed methods provide a robust and fully-automatic relative, absolute, and BBR accuracy assessment at sub-pixel level.

The results show that large relative shifts (up to 10 pixels) have occurred between consecutive HRV images (15 minutes interval) with Meteosat-8 during 1-19 February, 2008. The SEVIRI on Meteosat-9 delivers more stable images and the maximum relative shift is 1.4 pixels (slightly above the specification). The absolute accuracy values computed from the HRV images of 24 days acquired at 12:00 from both satellites show that shifts up to 1.5 pixels to the East and up to 3.3 pixels to the North are present. On the other side, another analysis on the Meteosat-8 images with large relative shifts has shown that these images have also large absolute geolocation errors (Aksakal et al., 2013). The mean absolute shifts obtained from 19 Meteosat-9 images are 0.9 (in x) and 2.3 (in y) pixels. The large relative shifts of Meteosat-8 images show that the geometric accuracy of these images are worse than the accuracy specifications by EUMETSAT. The inferior geometric accuracy and the occasional instability of the sensor should be taken into consideration for climate-related measurements and other applications of SEVIRI. The SEVIRI on Meteosat-9 delivers stable images and fulfills the relative and absolute accuracy specifications.

The absolute accuracy of the VIS 0.8 images are similar (in pixel) to the HRV images of the same acquisitions. Regarding the BBR accuracy between the VIS 0.8 and the 5 MS channels, no significant differences have been observed between Meteosat-8 and Meteosat-9. Both SEVIRI sensors have delivered images within the specifications given for the BBR accuracy. Similar investigations will be performed with the data of two other satellite sensors, namely MODIS and AVHRR.

ACKNOWLEDGMENTS

This study is supported by the Swiss GCOS Office at MeteoSwiss. The authors thank the members of the Swiss GCOS Office for providing data and their valuable inputs.

REFERENCES

- Aksakal, S.K., 2013. Geometric Accuracy Investigations of SEVIRI High Resolution Visible (HRV) Level 1.5 Imagery, *Remote Sensing*, **5**, 2475-2491; doi:10.3390/rs5052475.
- Aksakal, S.K., Baltasvias, E., Schindler, K., 2013. Analysis of the Geometric Accuracy of MSG-SEVIRI Imagery for Estimation of Climate Variables. 34th Asian Conference on Remote Sensing, Bali, Indonesia, 20-24 October (on CD-ROM, 8 p.).
- Aminou, D.M.A., Luhmann, H. J., Hanson, C., Pili, P., Jacquet, B., Bianchi, S., Coste, P., Pasternak, F., Faure, F., 2003. Meteosat Second Generation: A comparison of on-ground and on-flight imaging and radiometric performances of SEVIRI on MSG-1, *Proceedings of the 2003 EUMETSAT Meteorological Satellite Conference*, Weimar, Germany, 29 September-3 October, 236-243.
- Arnold, G.T., Hubanks, P.A., Platnick, S., King, M.D., Bennartz, R., 2010. Impact of Aqua Misregistration on MYD06 Cloud Retrieval Properties. Presented at *MODIS Science Team Meeting*, Washington, DC, USA, 26–28 January.
- Dürr, B., Zelenka, A., 2009. Deriving surface global irradiance over the Alpine region from Meteosat Second Generation by supplementing the HELIOSAT method, *International Journal of Remote Sensing*, **30**(22), 5821–5841, doi: 10.1080/01431160902744829.
- EUMETSAT, 2007, Typical Geometrical Accuracy for MSG-1/2, Doc. No: EUM/OPS/TEN/07/0313 v1, 26 February 2007.
- EUMETSAT, 2010, MSG Level 1.5 Image Data Format Description, Document No: EUM/MSG/ICD/105, Issue v6, 23 February 2010.
- GCOS, 2013. <http://www.wmo.int/pages/prog/gcos/> (accessed on 12.08.2013).
- Gieske, A.S.M., Hendrikse, J.H.M., Retsios, V., van Leeuwen, B., Maathuis, B.H.P., Romaguera, M., Sobrino, J.A., Timmermans, W.J., Su, Z., 2005. Processing of MSG - 1 SEVIRI data in the thermal infrared - algorithm development with the use of the SPARC2004 data set, *Proceedings of the ESA WPP-250 SPARC Final Workshop*, Enschede, The Netherlands, 4-5 July.
- Hanson, C., Mueller, J., 2004. Status of the SEVIRI Level 1.5 Data, *Proceedings of the Second MSG RAO Workshop* (ESA SP-582, November 2004), Salzburg, Austria, 9 - 10 September.
- Hanson, C.G., Mueller, J., Pili, P., Aminou, D.M.A., Jacquet, B., Bianchi, S., Coste, P., Faure, F., 2003. Meteosat Second Generation: SEVIRI Imaging Performance Results From The MSG-1 Commissioning Phase, *The 2003 EUMETSAT Meteorological Satellite Conference*, Weimar, Germany, 29 September-3 October.
- Just D., 2000. SEVIRI Level 1.5 Data, *Proceedings of the First MSG RAO Workshop* (ESA SP-452, October 2000), Bologna, Italy, 17-19 May.
- Lucas, B., Kanade, T., 1981. An Iterative Image Registration Technique with an Application to Stereo Vision. *Proceedings of 7th International Joint Conference on Artificial Intelligence (IJCAI)*, Vancouver, BC, Canada, 24–28 August.
- Seiz, G., Foppa, N., Meier, M., Paul, F., 2011. The role of satellite data within GCOS Switzerland, *Remote Sensing*, **3**, 767-780, doi: 10.3390/rs3040767.
- Swiss GCOS Office, 2013. GCOS Satellite Component, http://www.meteoschweiz.admin.ch/web/en/meteoswiss/international_affairs/gcos/Satellites.html (accessed on 11.10.2013).
- WMO, 2011. Systematic Observation Requirements for Satellite-based Products for Climate, Supplemental details to the satellite-based component of the Implementation Plan for the Global Observing System for Climate in Support of the UNFCCC (Update). Report, GCOS-154.